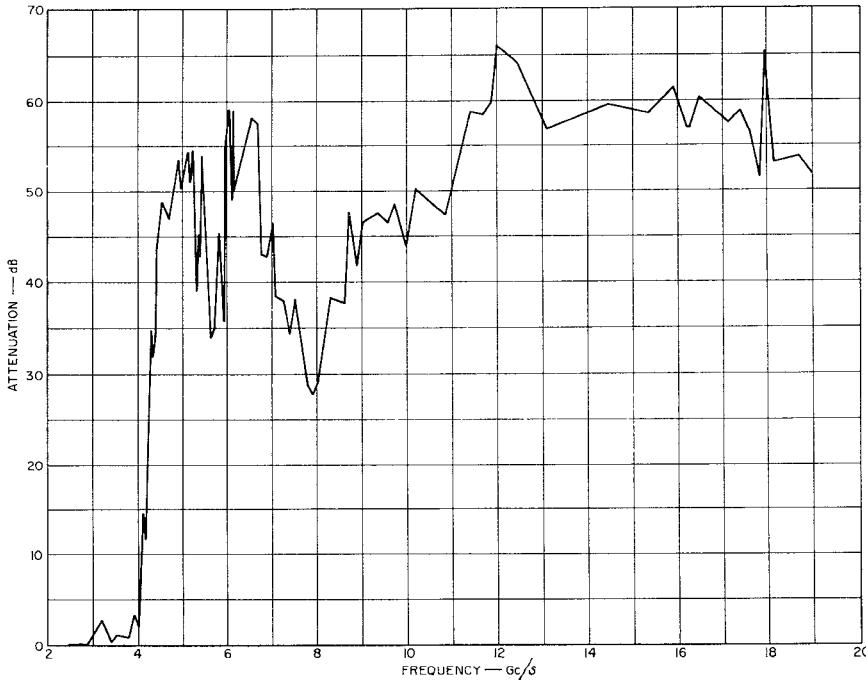


Fig. 3. VSWR and insertion loss in the pass-band of the filter of Fig. 2.

Fig. 4. Attenuation of the filter of Fig. 2 for the TE_{10} mode.

row band close to 8 Gc/s where the attenuation falls to about 27.5 dB. A tendency to a narrow spurious pass band (23-dB minimum attenuation) at about the same frequency was also found in the attenuation curve of the TE_{01} mode (not shown). The spurious response at 8 Gc/s, and other spurious responses could be reduced substantially by adding more side waveguides, with the septums placed in other positions than those shown in Fig. 1. The stop band is generally strong above this frequency for both the TE_{10} and TE_{01} modes and so confirms the

basic philosophy of this new filter configuration. The measured reflection coefficient for both the TE_{10} and TE_{01} modes tended to decrease with increasing frequency toward a value less than 0.01 at 19 Gc/s. The filter structure including the effects of input and output tapers was found to be fairly well matched throughout the stop band. Only in the transition region at about 4 Gc/s where the side waveguides do not yet propagate the TE_{10} mode, and the filter impedance is mismatched (because of the reactive filter effect in the periodic structure) to the waveguide

impedance, is there a reflection greater than half the input power. Below 2.9 Gc/s the measured reflection coefficient is below about -15 dB, in accordance with low measured VSWR (see Fig. 4).

A high-power test was made on the experimental filter. The available peak power was not enough to cause breakdown in the filter and the full peak power capability of this device is not known. However, it withstood 108 kW of peak pulse power with 2.6 μ s pulse length and 0.002 duty cycle at 2856 Mc/s, without any sign of arcing. It should be emphasized that these tests were made in air at atmospheric pressure.

CONCLUSION

Both the passband performance and stopband performance of the filter conform generally to what was predicted, but further work would be required to achieve the optimum results. Although the filter is low-pass from 2 to 4 Gc/s and has a sharp cutoff due to increasingly strong reactive effects at 4 Gc/s, the filter as constructed (Fig. 2) was matched only from 2.7 to 2.9 Gc/s, and no attempt was made to obtain a good match out to 4 Gc/s. Of particular interest is the fact that the attenuation in the stop band tends to increase with frequency, unlike conventional leaky-waveguide filters, which tend to lose their attenuation at the higher frequencies.

ACKNOWLEDGMENT

E. Fernandes very helpfully performed the many tedious measurements and adjustments on the trial filter.

B. M. SCHIFFMAN
LEO YOUNG
Stanford Research Inst.
Menlo Park, Calif.
G. L. MATTHAEI¹
Dept. of Elec. Engrg.
University of California
Santa Barbara, Calif.

REFERENCES

- [1] S. B. Cohn, "Design considerations for high-power microwave filters," *IRE Trans. on Microwave Theory*, vol. MTT-7, pp. 149-153, January 1959.
- [2] V. Met, "Absorptive filters for microwave harmonic power," *Proc. IRE*, vol. 47, pp. 1762-1769, October 1959.
- [3] V. G. Price, *et al.*, "Harmonic suppression by leaky-wall waveguide filter," *1959 IRE WESCON Conv. Rec.*, pt. 1, vol. 3, pp. 112-118.

¹ Formerly with Stanford Research Inst., Menlo Park, Calif.

Re-entrant Directional Coupler Using Strip Transmission Line

This correspondence describes a printed-circuit directional coupler design that is applicable to tight coupling (1 to 10 dB) values; it is a strip transmission line equivalent of the re-entrant coaxial coupler de-

scribed by Cohn.¹ Figure 1(a) shows the cross-sectional view of Cohn's device; the printed-circuit (strip transmission line) equivalent is shown in Fig. 1(b). The design of the coaxial version is determined by characteristic impedances Z_{01} (the impedance of a bar of width w and height b_2 placed within a ground plane spacing b_1) and Z_{02} (the impedance of the inner coaxial lines).

The printed-circuit version of the coupler is fabricated from commercially available copper-clad dielectric material and is designed to produce the same Z_{01} and Z_{02} values that are used in Fig. 1(a). The Z_{01} impedance is determined from the impedance of a metallic bar of width w_2 and height b_2 placed within a ground plane spacing b_1 . The Z_{02} value is obtained from the impedance of a strip of thickness t and width w_1 placed within a ground plane spacing b_2 . The two inner strips are assumed to be decoupled; $s/b_2 > 0.5$ satisfies this condition for a 3-dB coupler.

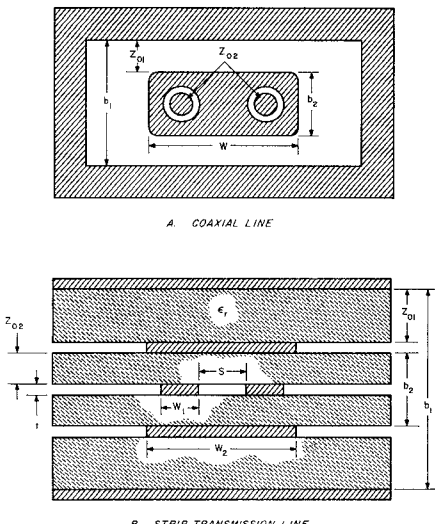


Fig. 1. Re-entrant cross sections.

A single-section 3-dB coupler using this technique was designed for the 450- to 850-Mc/s range. The experimental results are shown in Fig. 2. The coupling from ports 1 to 3 vs. frequency agrees with the theory within 0.15 dB; the SWR and isolation (insertion loss from ports 1 to 4) are comparable to values obtained with coaxial designs. The insertion loss between ports 1 and 2 is 0.25 dB higher than the theoretical; this is attributed to dissipation. These data were obtained with no experimental adjustments of the calculated parameters. This tends to demonstrate that no dimensionally critical spacings are required within the structure. This technique has been used successfully at frequencies as high as 4 Gc/s.

In summary, printed-circuit equivalents of Cohn's re-entrant coupler have been successfully designed and constructed. The tolerances inherent in the etching process are not serious in designs up to at least 4 Gc/s. The printed circuit version should, therefore, be inexpensive to produce and practical.

¹ S. B. Cohn, "Re-entrant cross section and wide-band 3-dB hybrid coupler," *IEEE Trans. on Microwave Theory and Techniques*, vol. MTT-11, pp. 254-258, July 1963.

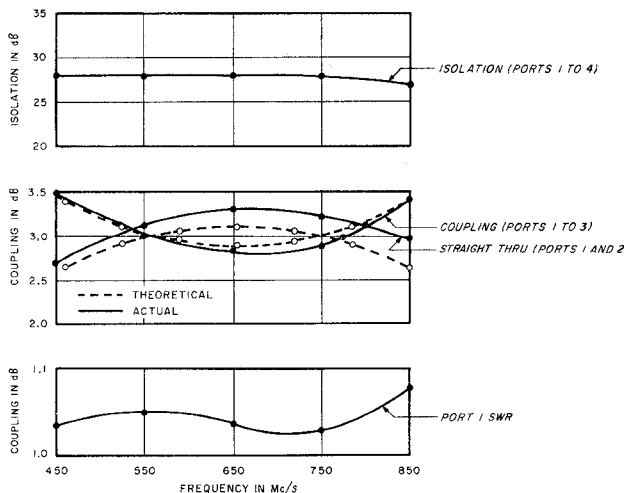


Fig. 2. Strip transmission line 3-dB re-entrant coupler.

to design to performance specifications comparable to that obtained with coaxial re-entrant couplers.

L. LAVENDOL
J. J. TAUB
Airborne Instruments Lab.
Cutler-Hammer, Inc.
Deer Park, N. Y.

for stable operation. The filter assembly, which was pressurized with 50 psig of air, experienced breakdown at 4.5-MW peak and 8.1-kW average. The threshold of breakdown for this unit was inaudible and could only be detected when seen through a viewing bend. When disassembled, burn marks were noted at the four corners of teeth in three center rows of waffle-iron I.

At this point in the program, consideration was given to a waffle-iron filter which utilized round teeth. This round tooth unit was a later version of the square tooth model [3] and was purported to improve the high power capability by a factor of 1.3. One such round tooth model of waffle I was fabricated and tested to a breakdown level of 4-MW peak and 7.1-kW average at 45 psig. This approach was dropped after assurances that breakdown was not due to extraneous causes.

To increase the high power capability of the square tooth filter, certain modifications were required. These modifications included: 1) an increase in tooth spacing and 2) a severe rounding of the teeth in the three center rows of waffle-iron I. The increase in tooth spacing of waffle-iron I resulted in a narrower stop band since the cutoff frequency of the filter was increased. The change of tooth surface area in waffle-iron I resulted in a capacitance reduction and a subsequent VSWR increase at the lower end of the pass band. No modifications were made to waffle-iron sections II and III.

Both of these modifications to waffle-iron I were made in incremental steps and each step was marked by an improvement in the high power handling capability of the filter assembly. This is shown in Fig. 2. It can be seen that a level of 6.7-MW peak and 12 kW of average power was achieved at 50 psig. This capability sufficed for the particular application; therefore, no effort was made to increase the power handling characteristics beyond this level. From Fig. 2 it can also be seen that waffle-iron section I limited the high power capability of the assembly. waffle-iron filters sections II and III were capable of higher power levels of 50 psig.

Figure 3 indicates the VSWR in the pass band for various conditions. Final VSWR data for the assembly, which included two